JPIS
Journal of Periodontal & Implant Science

Research Article
Implant Science

Check for updates

The healing pattern of a 4 mm proximal infrabony defect was not significantly different from a 2 mm defect adjacent to dental implant in a canine mandible

Min Kuk An [1,†], **Hyun Ju Kim** [1,2,†], **Jin Uk Choi** [1], **Kyoung-Hwa Kim** [1], **Yong-Moo Lee** [1], **In-Chul Rhyu** [1], **Yang-Jo Seol** [1,*]

[1]Department of Periodontology and Dental Research Institute, School of Dentistry, Seoul National University, Seoul, Korea
[2]Department of Periodontics, Seoul National University Dental Hospital, Seoul, Korea

*Correspondence:

Yang-Jo Seol

Department of Periodontology and Dental Research Institute, School of Dentistry, Seoul National University, 101 Daehak-ro, Jongno-gu, Seoul 03080, Korea.
Email: yjseol@snu.ac.kr
Tel: +82-2-2072-0308
Fax: +82-2-744-0051

†Min Kuk An and Hyun Ju Kim contributed equally to this work.

ORCID iDs
Min Kuk An
https://orcid.org/0000-0003-0932-4549
Hyun Ju Kim
https://orcid.org/0000-0002-9466-7126
Jin Uk Choi
https://orcid.org/0000-0003-1542-0588
Kyoung-Hwa Kim
https://orcid.org/0000-0001-5611-1242
Yong-Moo Lee
https://orcid.org/0000-0002-5619-3847
In-Chul Rhyu
https://orcid.org/0000-0003-4110-6381
Yang-Jo Seol
https://orcid.org/0000-0002-2076-5452

ABSTRACT

Purpose: The purpose of this study was to evaluate and compare the healing patterns of 2-mm and 4-mm proximal infrabony defects adjacent to dental implants in canine mandibles.
Methods: Four male beagles were used. Two groups were created: a 2-mm group (n=4) and a 4-mm group (n=4) depending on the horizontal dimension of proximal infrabony defects adjacent to implants. Bone healing patterns between the 2 groups were evaluated and compared at 8 and 16 weeks using radiographic, histological, histomorphometric, and fluorescent labelling analyses.
Results: According to microcomputed tomography, the median bone volume fraction, bone mineral density, and the percentage of radiographic distance from the defect bottom to the most coronal bone-to-implant contact (radio-mcBIC) were 32.9%, 0.6 g/cm³, and 73.7% (8 weeks) and 45.7%, 0.7 g/cm³, and 76.0% (16 weeks) in the 2-mm group and 57.7%, 0.8 g/cm³, and 75.7% (8 weeks) and 50.9%, 0.8 g/cm³, and 74.7% (16 weeks) in the 4-mm group, respectively. According to histomorphometry, the median bone area fraction, mcBIC and the percentage of BIC amounted to 36.7%, 3.4 mm, and 58.4% (8 weeks) and 49.2%, 3.4 mm, and 70.2% (16 weeks) in the 2-mm group and 50.0%, 3.0 mm, and 64.8% (8 weeks) and 55.7%, 3.0 mm, and 69.6% (16 weeks) in the 4-mm group, respectively. No statistically significant differences were found between the groups for any variables (*P*>0.05).
Conclusions: The proximal defects that measured 2 mm and 4 mm showed similar healing patterns at 8 and 16 weeks, and the top of bone formation in the defects was substantially limited to a maximum of 1.6 mm below the implant shoulder in both groups.

Keywords: Animal experimentation; Bone regeneration; Dental implants; Osseointegration; X-ray microtomography

Generated by xmlinkpress

Conflict of Interest

No potential conflict of interest relevant to this article was reported.

Authors Contributions

Conceptualization: Yang-Jo Seol; Formal analysis: Min Kuk An, Hyun Ju Kim, Yong-Moo Lee, In-Chul Rhyu; Investigation: Min Kuk An, Hyun Ju Kim, Kyoung-Hwa Kim; Methodology: Jin Uk Choi, In-Chul Rhyu, Kyoung-Hwa Kim; Project administration: Yang-Jo Seol; Writing - original draft: Min Kuk An, Hyun Ju Kim, Jin Uk Choi; Writing - review & editing: Kyoung-Hwa Kim, Yong-Moo Lee, In-Chul Rhyu, Yang-Jo Seol.

INTRODUCTION

It is well known that significant volumetric changes in the alveolar bone occur over time following tooth extraction [1-4]. A systematic review [3] reported that the horizontal dimension of the alveolar bone decreased by approximately 29% to 63% at 6 to 7 months after extraction, and the vertical dimension decreased by 11% to 22% at 6 months. A significant proportion of these volume changes occurred within 3 months of tooth extraction [3,5]. To minimise the early bone changes after tooth extraction and shorten the overall treatment time, there has been a great deal of interest and research on protocols for immediate or early implant placement [5-11]. Indeed, it is common for dental implants to be placed on an irregular bone contour before complete alveolar bone healing after extraction. When implants are placed into a fresh extraction socket or in the presence of irregular alveolar defects, defects of varying sizes often remain between the implant surface and the residual bone wall [12,13]. Large peri-implant defects that do not heal naturally can eventually lead to further bone loss or jeopardise implant stability and longevity [14]. It has been regarded that the most ideal healing pattern of infrabony defects adjacent to implants should exhibit optimal bone fill, with a large amount of bone-to-implant contact (BIC) and minimal resorption of the pre-existing bone [15]. Botticelli et al. [14] demonstrated that a circumferential gap of 1.25 mm around the implants could heal spontaneously with newly formed bone and obtain a similar degree of osseointegration as the implants in the control group, which were placed without a gap in a canine model. Several studies have shown that a 2-mm or smaller bone-to-implant defect can heal spontaneously with no regenerative procedure [13,15-17]. However, studies on the healing patterns of defects exceeding 2 mm are still limited, and most of them have focused on circumferential or horizontal buccal defects, not on defects in the proximal aspect [13,17-20].

If bone formation is not sufficient in the proximal infrabony defects adjacent to the implants, significant bone defects can remain, and osseointegration can also be compromised [21]. In addition, these defects can easily act as ecological niches of bacteria because the proximal area is susceptible to inflammation due to difficulty in cleansing (e.g., an interdental col area in the natural dentition) [22], which can lead to the progression of peri-implant bone loss [21,23]. Therefore, it is necessary to evaluate the healing pattern of proximal infrabony defects adjacent to the implants of varying sizes that heal spontaneously without leaving any unfavourable defects to prevent deterioration of the peri-implant tissue. Furthermore, such research could be used as a proof of concept to select a more desirable treatment modality between allowing for self-healing and performing gap filling with biomaterials, especially in managing large proximal infrabony defects.

The purpose of this pilot study was to evaluate and compare the healing pattern of 2-mm and 4-mm proximal infrabony defects adjacent to dental implants in canine mandibles. In this study, 2-mm and 4-mm infrabony defects were created at the mesial and distal sites of implants that were placed on the healed alveolar ridge. The patterns of spontaneous bone healing were then evaluated and compared at 8 and 16 weeks using radiographic, histological, histomorphometric, and fluorescent labelling analyses. The null hypothesis was that there would be no significant difference in the parameters representing bone healing patterns between 2-mm and 4-mm proximal infrabony defects adjacent to the implants.

MATERIALS AND METHODS

Animals and study design

This study was approved by the Institute of Laboratory Animal Resources (Seoul National University, South Korea, SNU-180605-1) and all procedures were performed in accordance with the guidelines established by the Seoul National University Institutional Animal Care and Use Committee and the Animal Research: Reporting In Vivo Experiments (ARRIVE) guidelines.

Four 12-month-old male beagles weighing 10–12 kg were enrolled in this study. During the experiment, all animals were housed individually in an animal facility at a laboratory animal centre at room temperature (23°C); the humidity was also controlled (60%) and dogs had *ad libitum* access to a standard dog diet. The groups were divided into a 2-mm group (n=4) and a 4-mm group (n=4) depending on the horizontal dimension of proximal infrabony defects adjacent to the dental implants. Each animal received 2 dental implants with 4 proximal infrabony defects (two 2-mm defects and two 4-mm defects). The bone healing patterns between the 2-mm group and the 4-mm group were evaluated and compared at 8 and 16 weeks. To ensure intact buccal and lingual bone walls around the defects, the 4-mm group needed to be allocated in the first molar area because of the narrow width of the buccolingual healed ridge in the premolar area. The timetable for the experimental protocol is schematically shown in **Figure 1**. The groups are described in **Figure 2A** and were as follows: 1) 2-mm group: 2-mm horizontal (bucco-lingual and mesio-distal) dimensions mesial or distal to the implant + 4-mm apico-coronal dimension of the defect; 2) 4-mm group: 4-mm horizontal (bucco-lingual and mesio-distal) dimensions mesial or distal to the implant + 4-mm apico-coronal dimension of the defect.

Surgical procedures

All surgical procedures were performed under general anaesthesia induced by an intravenous injection of a mixture of tiletamine/zolazepam (Zoletil, Virbac S.A., Carros, France) and xylazine hydrochloride (Rompun, Bayer AG, Leverkusen, Germany). Local infiltration anaesthesia using 2% lidocaine hydrochloride with 1:100,000 epinephrine (Lignospan; Septodont, Cedex, France) was additionally injected at the surgical sites.
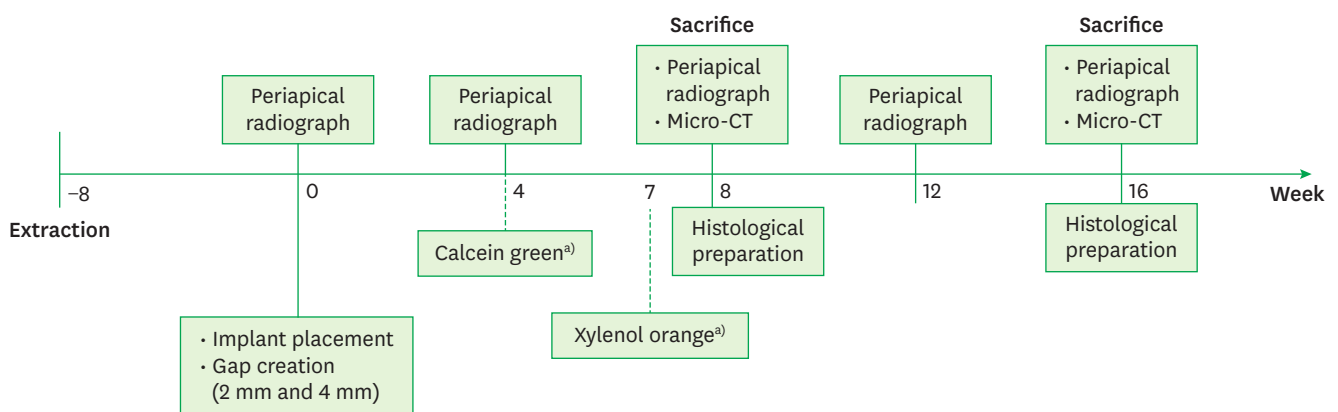

Figure 1. The timetable for all experimental protocols.
Micro-CT, micro-computed tomography.
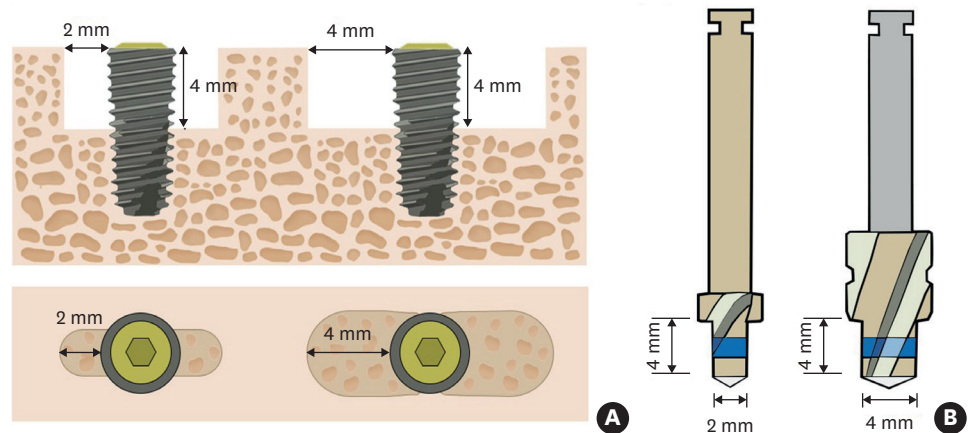[a)]Fluorescent calcium binding dyes.

Figure 2. The schematic figures showing the defects and the drills. (A) The defects of the 2-mm group (left) and the 4-mm group (right). (B) The designs of the customized drills used to create the proximal infrabony defects in the 2-mm group (left) and the 4-mm group (right).

First, the mandibular second, third, and fourth premolars (P2, P3, P4) and first molar (M1) of each animal were extracted. After 2 months of healing, a mucoperiosteal flap was elevated and the irregularly healed partially edentulous ridge was flattened and smoothened with a high-speed diamond bur (Tapered Chamfer Bur; Gebr. Brasseler GmbH & Co. KG, Lemgo, Germany). In the posterior region of the mandibular arch, 2 implant sites were prepared on the flattened ridge following a conventional drilling procedure under constant irrigation with sterile 0.9% saline solution for the placement of dental implants. The 2 created implant sites were located at a sufficient distance to avoid interfering with the formation of mesial and distal defects. Subsequently, 3-wall infrabony defects were created using customised drills (2 mm in diameter and 4 mm in length, 4 mm in diameter and 4 mm in length; Osstem Implant, Seoul, Korea; **Figure 2B**) mesial and distal to the prepared implant sites. All defects were created to allow for the existence of intact buccal and lingual walls. A dental implant (3.5 mm in diameter and 8.5 mm in length, SLA surface, internal hexagon [TSIII SA]; Osstem Implant) was placed on each prepared site, and the dimensions of the defects were verified with a periodontal probe (UNC 15; Hu-Friedy, Chicago, IL, USA). The horizontal dimension of the defects was 2 mm in the 2-mm group and 4 mm in the 4-mm group, and the length of the defect margin area was 4 mm in both groups (**Figure 2A**). All implants were placed so that the implant shoulder was located at the equicrestal position apico-coronally to the flattened crestal ridge. As for the buccolingual position, each implant was confirmed to have at least 1 mm of buccal and lingual bone thickness without any dehiscence, in order to avoid affecting the healing of the mesial and distal defects. After installation of the implants with good primary stability, cover screws were placed. The mucogingival flaps were repositioned and sutured with resorbable suture materials (5-0 chromic catgut; Taewoong Medical, Ilsan, Korea). All animals received an intramuscular injection of antibiotics (cefazolin, 30 mg/kg; Chong Kun Dang Pharmaceutical Corp., Seoul, Korea) to prevent postsurgical infections and were fed soft dog diets for 3 days following all surgical procedures. Representative clinical photographs of the surgical procedures are shown in **Figure 3**.

Serial periapical radiographs
Periapical radiographs were taken every 4 weeks during the entire experimental period for each implant to observe the changes in the mesio-distal bone level and contour following the creation of the mesio-distal defects.
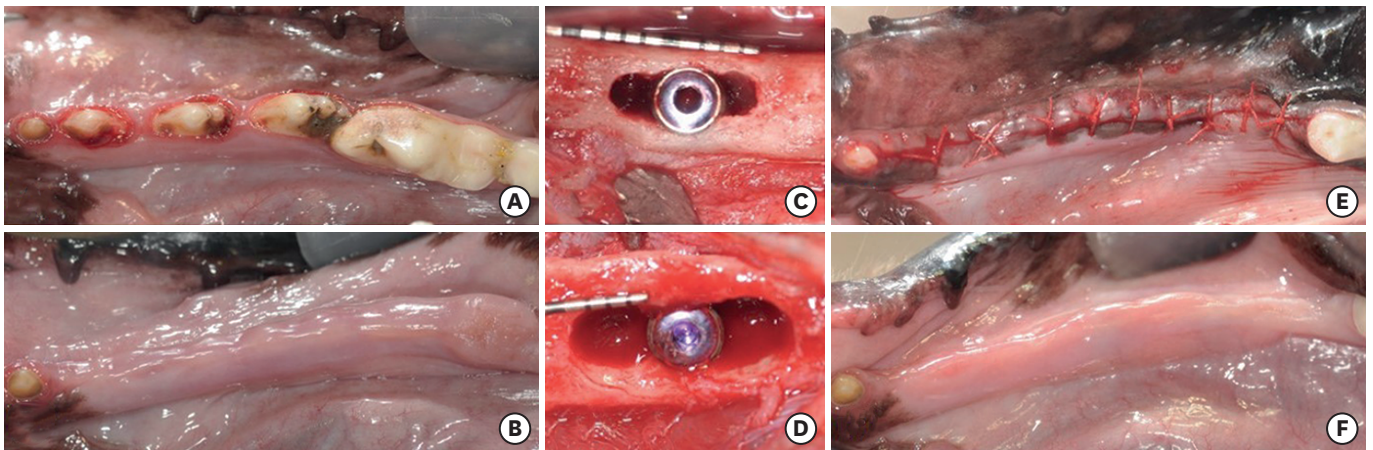
Figure 3. The representative clinical photographs for the surgical procedures. (A) Each animal initially showed full dentition. (B) P2, P3, P4, and M1 were extracted and the areas were allowed to heal for 2 months. An implant site was prepared and 3-wall infrabony defects were created mesial and distal to the prepared implant site. The implant was equicrestally placed and the dimensions of the defects were verified (C) 2-mm group and (D) 4-mm group. (E) The mucogingival flaps were repositioned and sutured. (F) After 8 and 16 weeks of healing, the animals were sacrificed.

Microcomputed tomographic analysis

The animals were euthanized 8 and 16 weeks after the creation of proximal infrabony defects adjacent to the implants, and the mandibles were harvested and fixed in 10% neutralised buffered formalin. Tissue samples from the mandible were scanned using a micro-computed tomography (micro-CT) scanner (SkyScan 1173; Bruker, Kontich, Belgium) at a resolution of 24 μm, and tomographic images were obtained at 130 kV and 60 μA. These images were visualised and converted into a suitable dataset with appropriate orientation and axes using micro-CT visualisation software (DataViewer; Bruker) to perform the main quantitative measurements. The regions of interest (ROIs) for the micro-CT data and the reference lines for the measurements are shown in **Figure 4A-E**.

The following parameters were quantified for each defect on the mesial and distal aspects of the implants using analytical software (CTAn; Bruker) applying adaptive thresholding with a pre-threshold level of 23: 1) the percentage of bone volume per total tissue volume (BV/TV; %); 2) bone mineral density (BMD; g/cm^3); 3) the percentage of bone area per tissue area measured in the micro-CT sectional view bisecting each defect to the mesio-distal plane (radio-BA/TA; %); and 4) the percentage of the radiographic distance from the bottom of the original defect to the most coronal level of BIC per original defect length, which was measured parallel to the long axis of the implant (radio-mcBIC; %).

Histological preparation and histomorphometrical analysis

The tissue samples were dehydrated and embedded in methyl methacrylate (Technovit 7200; Exakt, Hamburg, Germany). Undecalcified sections bisecting the implant in a mesio-distal direction were prepared using a cutting-grinding unit (Exakt Apparatebau, Norderstedt, Germany). A multiple stain solution (Polyscience, Inc., Warrington, PA, USA) was used to stain the microscopic slides. Histological examinations were performed by observing the stained sections using a light microscope (Olympus BX 50; Olympus Optical, Osaka, Japan), and each slide was photographed with a digital camera. Histomorphometric analyses were performed using digital image analysis software (ImageJ; U.S. National Institutes of Health, Bethesda, MD, USA) and detailed by freehand drawing. All histomorphometrical measurements were taken by an experienced examiner (JUC) in a blinded manner in triplicate and were averaged. The ROIs for the histomorphometric measurements are shown in **Figure 4F and G**. The following
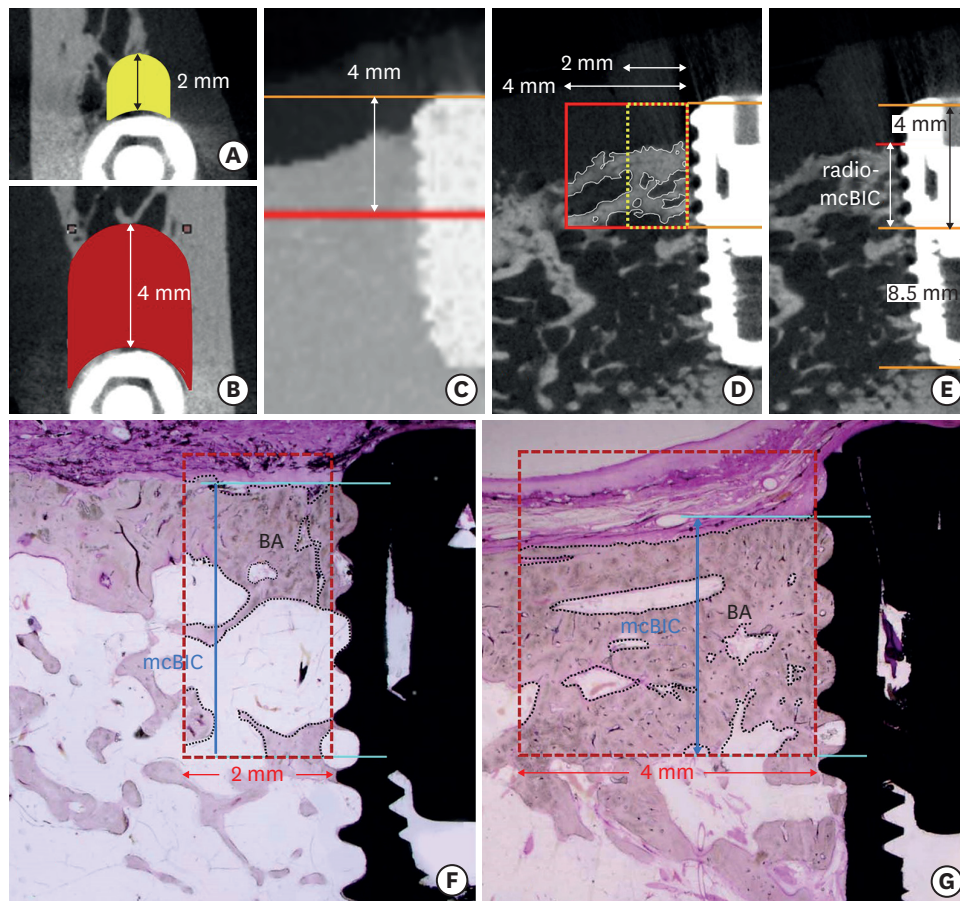
Figure 4. The ROIs for the micro-CT measurements (A-E) and the histomorphometric measurements (F, G) and their reference lines. The ROI for the measurements of BV/TV and BMD in the 2-mm group (A) and the 4-mm group (B), shown in a transverse view, and the length of ROIs (C) in a mesio-distal sectional view. (D) ROIs showing radio-BA/TA: the square outlined with a dotted yellow line indicates the ROI for the 2-mm group and the one with a solid red line indicates the ROI for the 4-mm group. (E) Mesio-distal sectional view showing the radio-mcBIC: the solid red line indicates the level of the most coronal radiographic BIC and the orange reference lines depict the level of implant shoulder, the bottom of the defect and implant apex from the top, respectively. The ROIs for the histomorphometric measurements and the reference lines: the squares outlined with dotted red lines depict the ROI for the measurement of BA/TA in the 2-mm group (F) and the 4-mm group (G). The solid sky-blue lines indicate the levels of the most coronal BIC and the bottom of the original defect from the top, respectively. The length of mcBIC was measured from the bottom of the defect to the most coronal level of BIC (blue double-sided arrow).

ROI: region of interest, BV/TV: bone volume per total tissue volume, BMD: bone mineral density, radio-BA/TA: radiographically measured bone area per tissue area, BIC: bone-implant contact, radio-mcBIC: radiographic distance from the bottom of the original defect to the most coronal level of BIC per original defect length.

parameters were measured for each defect on the mesial and distal aspects of the implants: 1) the area of regenerated bone (BA; mm²); 2) the percentage of the area of regenerated bone per total tissue area (BA/TA; %); 3) the distance from the bottom of the original defect to the most coronal level of the BIC, which was measured parallel to the long axis of the implant (mcBIC; mm); and 4) the percentage of the BIC to the total surface of the threaded implant (%BIC; %).

Fluorescent labelling analysis

Fluorescent calcium-binding dyes were injected subcutaneously into all animals to identify new bone formation and bone remodelling over time. Calcein green (10 mg/kg; Sigma, St. Louis, MO, USA) was injected after 4 weeks, and xylenol orange (90 mg/kg; Sigma) was administered 7 weeks after defect creation. Unstained ground sections were used to analyse fluorescent labelling, which was visualised using a fluorescence microscope (Olympus Optical) and photographed with a built-in digital camera.

Statistical analysis

All statistical analyses were performed using commercially available software (SPSS 26; IBM Corp., Armonk, NY, USA) and Microsoft Excel (Microsoft Corp., Redmond, WA, USA). The quantitative variables were described as the median with quartiles (Q1: 25th percentile, Q3: 75th percentile) and the mean and standard deviation. The Wilcoxon signed-rank test was performed to evaluate the differences between the 2 groups, since each defect group was assigned on each animal's mandible evenly. Statistical significance was set at $P<0.05$.

RESULTS

None of the animals showed any signs of postoperative infection or any eventful complications, including wounds, dehiscence, implant exposure, or other systemic problems throughout the study period.

Serial periapical radiographic findings

The mesial and distal defects in all groups showed an increase in radiopacity on periapical radiographs over time (**Figure 5**). The 2-mm group showed radiopacity similar to that of
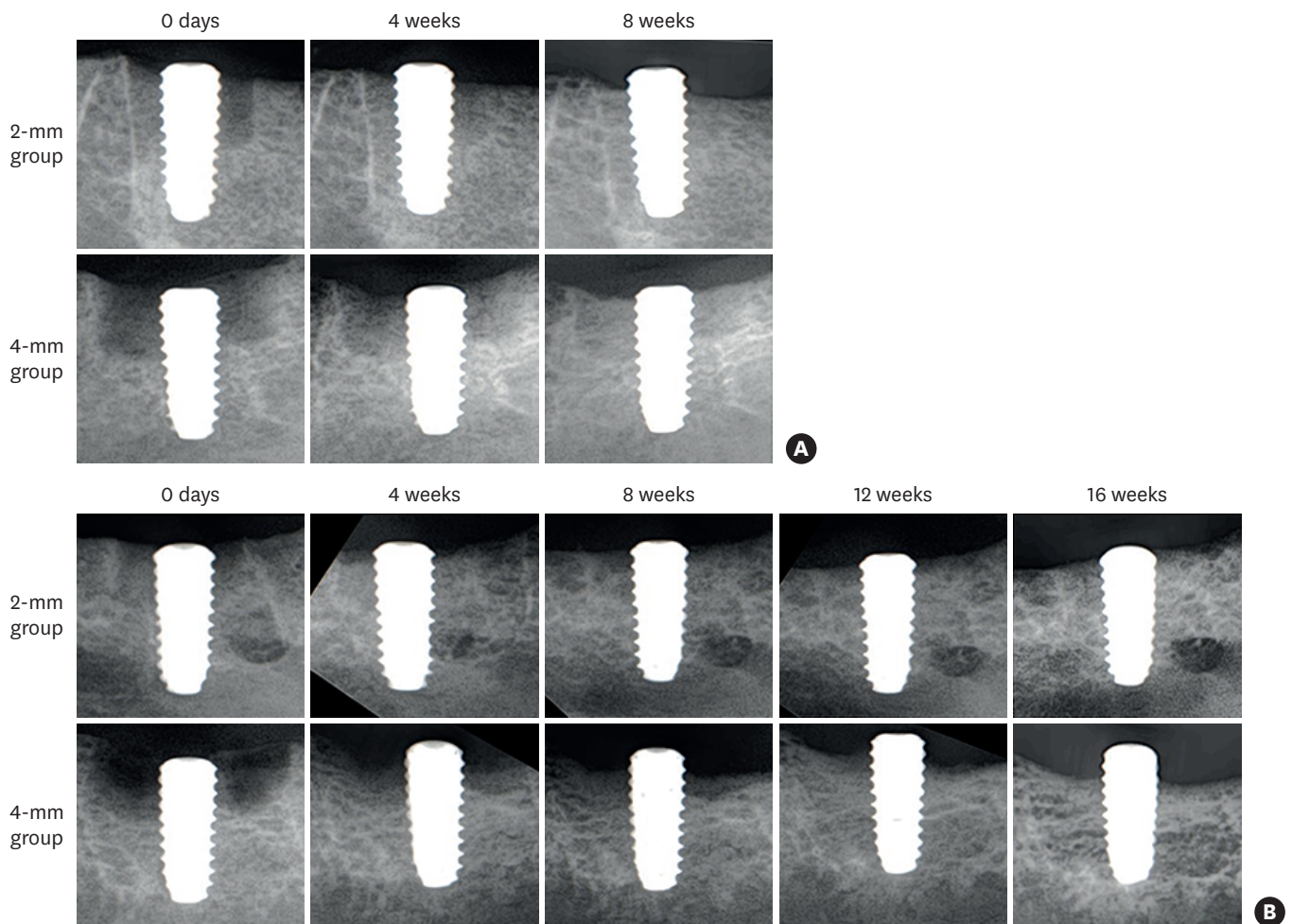

Figure 5. Representative serial periapical radiographs of the 2-mm and 4-mm groups. Radiographs of the animals sacrificed at 8 weeks (A) and 16 weeks (B). The radiolucency of the defects disappeared and was well-harmonised with the adjacent old bone at 16 weeks.

the adjacent old bone, with the defect margin indiscernible starting at 8 weeks. However, the 4-mm group still had radiolucency inside the defect at 8 weeks; the defect margin was discernible, and the relative radiolucency lasted until 12 weeks.

In both groups, the most coronal radiographic BIC was close to the implant shoulder or located within the first to the second thread (less than 1.6 mm) from the implant shoulder, although there were individual differences between animals. The degree of exposure of the infrabony component (SLA surface) of the fixtures was more pronounced in the 4-mm group.

Microcomputed tomographic analysis

Table 1 shows the BV/TV (%), BMD (g/cm^3), radio-BA/TA (%), and radio-mcBIC (%) results evaluated using micro-CT at 8 and 16 weeks after defect creation. There were no significant differences between the 2-mm and the 4-mm groups regarding all variables ($P>0.05$).

At 8 weeks, the median values (Q1–Q3) of the BV/TV, BMD, radio-BA/TA, and radio-mcBIC in the 2-mm group amounted to 32.9% (30.1%–35.3%), 0.6 g/cm^3 (0.5–0.6 g/cm^3), 24.8% (23.7%–26.8%), and 73.7% (67.4%–81.7%), respectively. In the 4-mm group, the respective median values at 8 weeks amounted to 57.7% (47.8%–61.6%), 0.8 g/cm^3 (0.7–0.9 g/cm^3), 59.6% (50.8%–63.3%), and 75.7% (65.4%–87.0%). Of note, the 4-mm group exhibited a tendency for higher values with respect to all variables than those of the 2-mm group at 8 weeks.

At 16 weeks, the median values (Q1–Q3) of the BV/TV, BMD, radio-BA/TA, and radio-mcBIC in the 2-mm group amounted to 45.7% (40.2%–52.0%), 0.7 g/cm^3 (0.6–0.8 g/cm^3), 38.7% (29.7%–47.8%), and 76.0% (72.6%–80.1%), respectively. In the 4-mm group, the respective median values at 16 weeks amounted to 50.9% (44.1%–57.5%), 0.8 g/cm^3 (0.7–0.9 g/cm^3), 46.1% (44.1%–50.1%), and 74.7% (68.9%–80.2%). At 16 weeks of healing as well, the 4-mm group exhibited a tendency for higher values regarding the values of BV/TV, BMD, and radio-BA/TA than those of the 2-mm group.

Histological findings and fluorescent labelling analysis

Osseointegration was well established in all implants. **Figure 6** shows representative histological and matching fluorescent images corresponding to each group at 8 and 16 weeks after defect creation. All implants were well covered with soft tissue without exposure of the cover screws. The most coronal BIC was very close to the implant shoulder without exposure of the implant thread (**Figure 6E**) or was only located within the first to the second thread (less than 1.6 mm from the implant shoulder) in both groups (**Figure 6A, C, and G**), if any. Peri-

Table 1. The results of the micro-CT analysis

Healing period	Variable	2-mm group	4-mm group	P-value[a]
8 weeks	BV/TV (%)	32.9 (30.1–35.3)	57.7 (47.8–61.6)	0.125
	BMD (g/cm^3)	0.6 (0.5–0.6)	0.8 (0.7–0.9)	0.188
	radio-BA/TA (%)	24.8 (23.7–26.8)	59.6 (50.8–63.3)	0.063
	radio-mcBIC (%)	73.7 (67.4–81.7)	75.7 (65.4–87.0)	0.438
16 weeks	BV/TV (%)	45.7 (40.2–52.0)	50.9 (44.1–57.5)	0.313
	BMD (g/cm^3)	0.7 (0.6–0.8)	0.8 (0.7–0.9)	0.313
	radio-BA/TA (%)	38.7 (29.7–47.8)	46.1 (44.1–50.1)	0.188
	radio-mcBIC (%)	76.0 (72.6–80.1)	74.7 (68.9–80.2)	0.188

The quantitative variables were described as the median with quartiles (Q1–Q3).
Micro-CT: microcomputed tomography; BV/TV: bone volume per total tissue volume, BMD: bone mineral density, radio-BA/TA: radiographically measured bone area per tissue area, radio-mcBIC: radiographic distance from the bottom of the original defect to the most coronal level of bone-implant contact per original defect length, Q1: 25th percentile value, Q3: 75th percentile value.
[a]P-value evaluated by the Wilcoxon signed rank test. P-values less than 0.05 were considered statistically significant.
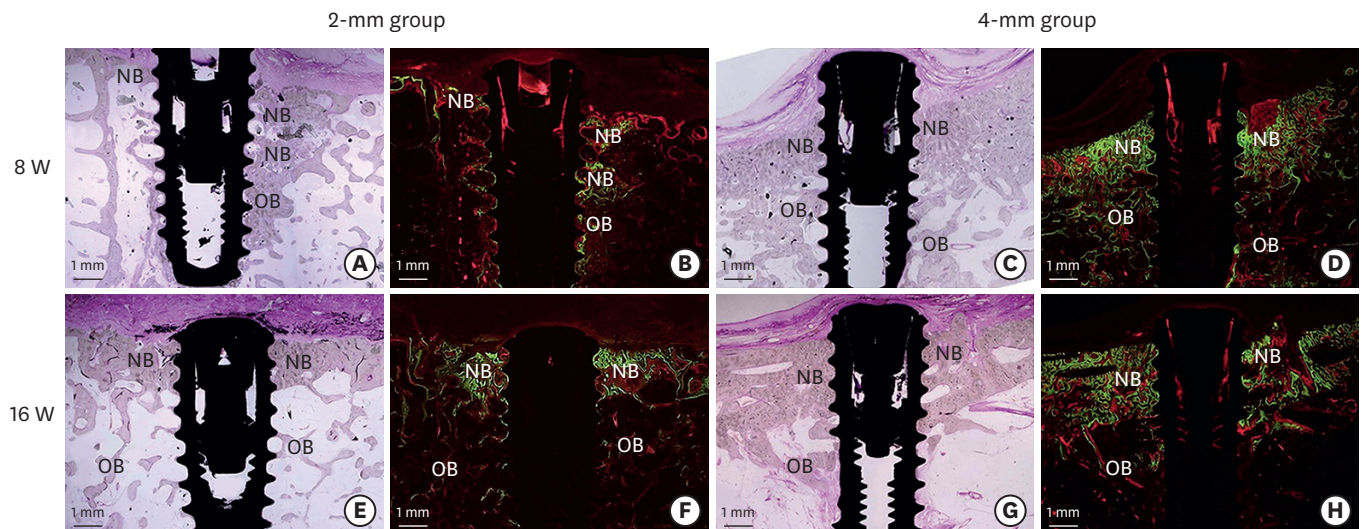
Figure 6. The representative histological (A, C, E, G; haematoxylin and eosin staining) and the matching fluorescent images (B, D, F, H; calcein green, xylenol orange). The green colour represents the new bone apposition labelled by calcein after 4 weeks and the orange colour represents labelling by xylenol after 7 weeks. NB: new bone, OB: old bone, W: weeks.

implant bone concavity, possibly indicating remaining infrabony defects, was not observed in either group, and the superior border of the crestal bone was horizontally well-contoured. The newly formed bone showed highly calcified tissue compared to the adjacent old bone, and the new bone tissue in the 4-mm group exhibited less bone marrow space and appeared denser, with a more compact pattern, than that in the 2-mm group at both time points. The apical half of the original defect in the 2-mm group exhibited good harmony with the adjacent old bone, showing a larger amount of marrow spaces than the upper half of the defect.

New bone formation was observed in the fluorescent images by calcein green and xylenol orange labels in all samples. In the fluorescent images, more accentuated fluorescent labelling was observed for calcein green than for xylenol orange in all groups. In addition, the labelling of new bone tissue that comprised the BIC of the original infrabony defect was mostly reflected by calcein green. However, fluorescent labelling by xylenol orange showed a slightly scattered pattern that was rarely observed in the BIC area.

Histomorphometrical analysis

Table 2 shows the BA/TA (%), mcBIC (mm), and %BIC (%) results of histomorphometric analysis at 8 and 16 weeks after defect creation. There was no significant difference between the 2-mm and 4-mm groups regarding all variables ($P>0.05$).

Table 2. The results of the histomorphometric analysis

Healing period	Variable	2-mm group	4-mm group	P-value[a]
8 weeks	BA/TA (%)	36.7 (34.1–37.0)	50.0 (42.1–55.3)	0.125
	mcBIC (mm)	3.4 (2.9–3.8)	3.0 (2.4–3.7)	0.250
	%BIC (%)	58.4 (54.5–65.9)	64.8 (61.4–70.8)	0.313
16 weeks	BA/TA (%)	49.2 (45.0–52.9)	55.7 (53.2–57.4)	0.063
	mcBIC (mm)	3.4 (3.0–3.6)	3.0 (2.8–3.3)	0.438
	%BIC (%)	70.2 (66.0–73.7)	69.6 (63.2–74.2)	0.563

The quantitative variables were described as the median with quartiles (Q1–Q3).
BA/TA: area of regenerated bone per total tissue area, mcBIC: the distance from the bottom of the original defect to the most coronal level of the bone-to-implant contact, %BIC: bone-to-implant contact to the total surface of the threaded implant, Q1: 25th percentile value, Q3: 75th percentile value.
[a]P-value evaluated by the Wilcoxon signed rank test. P-values less than 0.05 were considered statistically significant.

Of note, the 4-mm group showed a tendency for higher median BA/TA values (Q1–Q3) in both healing periods, although it did not reach statistical significance (2-mm group at 8 weeks: 36.7% [34.1%–37.0%] vs. the 4-mm group at 8 weeks: 50.0% [42.1%–55.3%]; 2-mm group at 16 weeks: 49.2% [45.0%–52.9%] vs. 4-mm group at 16 weeks: 55.7% [53.2%–57.4%]). In contrast, as for the mcBIC (mm) indicating the distance from the bottom of the original defect to the highest BIC point, the 2-mm group showed a tendency for slightly higher median values at both time points (2-mm group at 8 weeks: 3.4 mm [2.9–3.8 mm] vs. 4-mm group at 8 weeks: 3.0 mm [2.4–3.7 mm]; 2-mm group at 16 weeks: 3.4 mm [3.0–3.6 mm] vs. 4-mm group at 16 weeks: 3.0 mm [2.8–3.3 mm]). The median %BIC values amounted to 58.4% [54.5%–65.9%] for the 2-mm group and 64.8% [61.4%–70.8%] for the 4-mm group at 8 weeks, and 70.2% [66.0%–73.7%] and 69.6% [63.2%–74.2%] for the 2-mm and 4-mm groups at 16 weeks, respectively ($P>0.05$).

DISCUSSION

The aim of this study was to evaluate and compare the healing pattern of 2-mm and 4-mm proximal infrabony defects adjacent to dental implants in a canine mandible. The null hypothesis was that there would be no significant difference with respect to the variables representing the bone healing patterns of the defects between 2 groups, and in this study the hypothesis was supported through the radiographic, histologic, histomorphometric, and fluorescent labelling analyses.

It was revealed that there were no significant differences between the 2 groups in terms of BV/TV (%), BMD (g/cm³), radio-BA/TA (%), and radio-mcBIC (%) from the micro-CT analysis and BA/TA (%), mcBIC (mm), and %BIC (%) from the histomorphometric analysis at 8 and 16 weeks. Serial periapical radiographs revealed that marked bone filling was achieved in both groups, showing an increase in radiopacity within the defect area over time. The histological slides also showed a horizontally well-remodelled alveolar bone crest in both groups. As for the BIC, the most coronal radiographic and histologic BIC were close to the implant shoulder or were located within the first to the second thread (a maximum of 1.6 mm below the implant shoulder) in both groups. In the fluorescent labelled images, new bone formation was clearly visible, as there were calcein green and xylenol orange labels within the defect area in all samples of both groups. These results indicate that the spontaneous bone healing pattern and degree of osseointegration of 4-mm proximal infrabony defects were similar to those of 2-mm defects in the canine mandible.

In the current study, the 4-mm group exhibited a tendency for higher values in the parameters of BV/TV, BMD, and radio-BA/TA from the micro-CT analysis and BA/TA from the histomorphometric analysis than those of the 2-mm group at both time points. The parameters with higher values in the 4-mm group are known to be associated with the amount of mineralized or calcified tissue. This can likely be attributed to early bone remodelling and maturation of the newly formed bone in the 2-mm group. It has been shown that bone marrow spaces increase as bone maturation progresses [24]. Moreover, as maturation progresses, the boundary with pre-existing old bone becomes indistinguishable and well-harmonised with the new bone [25,26]. These results are also supported by the histological results in the current study. According to the histological findings, the new bone tissue in the 4-mm group exhibited less marrow space and appeared denser, with a more compact pattern of calcified tissue, than that in the 2-mm group at both time points.

The apical half of the original defects in the 2-mm group exhibited good harmony with the adjacent old bone, showing a larger amount of marrow space than the upper half of the defect, suggesting that bone maturation occurred first in the area in this group.

Al-Sabbagh and Kutkut [16] reported that a bone-to-implant defect of less than 2 mm did not affect implant stability without any regenerative procedures in human clinical studies. In another prospective randomised clinical study, the amount of hard and soft tissue changes was similar when the healing pattern of a horizontal gap less than 2 mm was compared to the healing of the gap where the bone graft was performed [17]. In agreement with previous studies, in the current study, the histological and histomorphometric evidence demonstrated that the proximal infrabony defects adjacent to implants resolved well, showing considerable bone filling and an acceptable degree of BIC.

In the fluorescent labelling analysis, the newly formed bone was primarily labelled by calcein and the bone tissue comprising the BIC of the previously created defect was also labelled primarily by calcein green in both groups. The incorporated pattern of calcein green administered at 4 weeks was dense and compact, whereas that of xylenol orange injected at 7 weeks was slightly scattered. These findings indicated that a considerable volume of bone had already been formed at 4 weeks, and additional bone formation and remodelling were observed at 7 weeks.

According to our results, resolution of the infrabony defects was achieved; however, for some samples in both groups, bone formation in the defects was limited to a maximum of 1.6 mm below the implant shoulder, substantially exposing threads above the crestal bone. It is not yet clear whether this was due to space collapse caused by the inherent limitation of canine models, which lack compliance compared to human studies, or physiological bone loss corresponding to buccal bone resorption, as reported in some previous studies that examined buccal gaps [27-29]. Although there can be a considerable difference between the results of animal studies and clinical results, this preclinical study revealed that 4-mm proximal infrabony defects could be acceptably managed and resolved, similarly to 2-mm defects adjacent to the implant. Considering the subsequent alveolar bone remodelling based on the current evidence, the authors cautiously recommend placing an implant approximately 1.6 mm deep inside the alveolar bone to prevent the intrabony component of implants from being exposed above the level of the alveolar crest. Otherwise, gap filling with biomaterials could be recommended for immediate or early implant placement on sites having these types of proximal infrabony defects.

Despite several new findings, the current study has some limitations, such as the small sample size and statistical limits. In addition, our implant placement protocols did not exactly simulate an immediate or early implant placement protocol. We used a delayed implant placement protocol and primary closure, which would be helpful for blood clot stabilisation and initial healing. Furthermore, this study was designed so that the 2-mm group was allocated at the premolar region and the 4-mm group at the molar region—that is, the defect sites were not randomised. Further well-designed, randomised human studies with or without gap-filling biomaterials on the management of large proximal infrabony defects adjacent to the implants are necessary.

In conclusion, the proximal defects in both groups showed similar healing patterns at 8 and 16 weeks, and the top of bone formation in the defects was substantially limited to a maximum of 1.6 mm below the implant shoulder in both groups.

ACKNOWLEDGEMENTS

REFERENCES

1. Mardas N, Chadha V, Donos N. Alveolar ridge preservation with guided bone regeneration and a synthetic bone substitute or a bovine-derived xenograft: a randomized, controlled clinical trial. Clin Oral Implants Res 2010;21:688-98.
   PUBMED | **CROSSREF**

2. Shi B, Zhou Y, Wang YN, Cheng XR. Alveolar ridge preservation prior to implant placement with surgical-grade calcium sulfate and platelet-rich plasma: a pilot study in a canine model. Int J Oral Maxillofac Implants 2007;22:656-65.
   PUBMED

3. Tan WL, Wong TL, Wong MC, Lang NP. A systematic review of post-extractional alveolar hard and soft tissue dimensional changes in humans. Clin Oral Implants Res 2012;23 Suppl 5:1-21.
   PUBMED | **CROSSREF**

4. Brkovic BM, Prasad HS, Rohrer MD, Konandreas G, Agrogiannis G, Antunovic D, et al. Beta-tricalcium phosphate/type I collagen cones with or without a barrier membrane in human extraction socket healing: clinical, histologic, histomorphometric, and immunohistochemical evaluation. Clin Oral Investig 2012;16:581-90.
   PUBMED | **CROSSREF**

5. Schropp L, Wenzel A, Kostopoulos L, Karring T. Bone healing and soft tissue contour changes following single-tooth extraction: a clinical and radiographic 12-month prospective study. Int J Periodontics Restorative Dent 2003;23:313-23.
   PUBMED

6. Altintas NY, Taskesen F, Bagis B, Baltacioglu E, Cezairli B, Senel FC. Immediate implant placement in fresh sockets versus implant placement in healed bone for full-arch fixed prostheses with conventional loading. Int J Oral Maxillofac Implants 2016;45:226-31.
   PUBMED | **CROSSREF**

7. Chen ST, Buser D. Clinical and esthetic outcomes of implants placed in postextraction sites. Int J Oral Maxillofac Implants 2009;24 Suppl:186-217.
   PUBMED

8. Watzek G, Haider R, Mensdorff-Pouilly N, Haas R. Immediate and delayed implantation for complete restoration of the jaw following extraction of all residual teeth: a retrospective study comparing different types of serial immediate implantation. Int J Oral Maxillofac Implants 1995;10:561-7.
   PUBMED

9. Schropp L, Kostopoulos L, Wenzel A. Bone healing following immediate versus delayed placement of titanium implants into extraction sockets: a prospective clinical study. Int J Oral Maxillofac Implants 2003;18:189-99.
   PUBMED

10. Chen ST, Buser D. Esthetic outcomes following immediate and early implant placement in the anterior maxilla--a systematic review. Int J Oral Maxillofac Implants 2014;29 Suppl:186-215.
    PUBMED | **CROSSREF**

11. Hämmerle CH, Chen ST, Wilson TG Jr. Consensus statements and recommended clinical procedures regarding the placement of implants in extraction sockets. Int J Oral Maxillofac Implants 2004;19 Suppl:26-8.
    PUBMED

12. Jacobs BP, Zadeh HH, De Kok I, Cooper L. A randomized controlled trial evaluating grafting the facial gap at immediately placed implants. Int J Periodont Restor Dent 2020;40:383-92.
    PUBMED | **CROSSREF**

13. Naji BM, Abdelsameaa SS, Alqutaibi AY, Said Ahmed WM. Immediate dental implant placement with a horizontal gap more than two millimetres: a randomized clinical trial. Int J Oral Maxillofac Implants 2021;50:683-90.
    PUBMED | **CROSSREF**

14. Botticelli D, Berglundh T, Buser D, Lindhe J. The jumping distance revisited: an experimental study in the dog. Clin Oral Implants Res 2003;14:35-42.
    PUBMED | **CROSSREF**

15. Greenstein G, Cavallaro J. Managing the buccal gap and plate of bone: immediate dental implant placement. Dent Today 2013;32:70, 72-7.
PUBMED

16. Al-Sabbagh M, Kutkut A. Immediate implant placement: surgical techniques for prevention and management of complications. Dent Clin North Am 2015;59:73-95.
PUBMED | CROSSREF

17. Kabi S, Kar R, Samal D, Deepak KC, Kar IB, Mishra N. Immediate dental implant placement with or without autogenous bone graft: a comparative study. Natl J Maxillofac Surg 2020;11:46-52.
PUBMED | CROSSREF

18. Tarnow DP, Chu SJ. Human histologic verification of osseointegration of an immediate implant placed into a fresh extraction socket with excessive gap distance without primary flap closure, graft, or membrane: a case report. Int J Periodont Restor Dent 2011;31:515-21.
PUBMED

19. Dos Santos PL, de Molon RS, Queiroz TP, Okamoto R, de Souza Faloni AP, Gulinelli JL, et al. Evaluation of bone substitutes for treatment of peri-implant bone defects: biomechanical, histological, and immunohistochemical analyses in the rabbit tibia. J Periodontal Implant Sci 2016;46:176-96.
PUBMED | CROSSREF

20. Wilson TG Jr, Schenk R, Buser D, Cochran D. Implants placed in immediate extraction sites: a report of histologic and histometric analyses of human biopsies. Int J Oral Maxillofac Implants 1998;13:333-41.
PUBMED

21. Gomez-Roman G. Influence of flap design on peri-implant interproximal crestal bone loss around single-tooth implants. Int J Oral Maxillofac Implants 2001;16:61-7.
PUBMED

22. Takei HH. The interdental space. Dent Clin North Am 1980;24:169-76.
PUBMED | CROSSREF

23. Buser D, Martin W, Belser UC. Optimizing esthetics for implant restorations in the anterior maxilla: anatomic and surgical considerations. Int J Oral Maxillofac Implants 2004;19 Suppl:43-61.
PUBMED

24. Chakar C, Naaman N, Soffer E, Cohen N, El Osta N, Petite H, et al. Bone formation with deproteinized bovine bone mineral or biphasic calcium phosphate in the presence of autologous platelet lysate: comparative investigation in rabbit. Int J Biomater 2014;2014:367265.
PUBMED | CROSSREF

25. Kajii F, Iwai A, Tanaka H, Matsui K, Kawai T, Kamakura S. Single-dose local administration of teriparatide with a octacalcium phosphate collagen composite enhances bone regeneration in a rodent critical-sized calvarial defect. J Biomed Mater Res B Appl Biomater 2018;106:1851-7.
PUBMED | CROSSREF

26. Omar O, Engstrand T, Kihlström Burenstam Linder L, Åberg J, Shah FA, Palmquist A, et al. In situ bone regeneration of large cranial defects using synthetic ceramic implants with a tailored composition and design. Proc Natl Acad Sci U S A 2020;117:26660-71.
PUBMED | CROSSREF

27. Degidi M, Daprile G, Nardi D, Piattelli A. Buccal bone plate in immediately placed and restored implant with Bio-Oss® collagen graft: a 1-year follow-up study. Clin Oral Implants Res 2013;24:1201-5.
PUBMED | CROSSREF

28. Sanz M, Lindhe J, Alcaraz J, Sanz-Sanchez I, Cecchinato D. The effect of placing a bone replacement graft in the gap at immediately placed implants: a randomized clinical trial. Clin Oral Implants Res 2017;28:902-10.
PUBMED | CROSSREF

29. Blanco J, Carral C, Argibay O, Liñares A. Implant placement in fresh extraction sockets. Periodontol 2000 2019;79:151-67.
PUBMED | CROSSREF